# Photons fluence to local skin Dose coefficients and benchmark with three Monte-Carlo codes. Application to the computation of radioactive material transport limits

Thomas Frosio, Philippe Bertreix, Nabil Menaa, Janis Endres, Samuel Thomas, Holger Eberhardt

Applied Radiation and Isotopes 176 (2021) 109892

Contents lists available at ScienceDirect

Applied Radiation and Isotopes

journal homepage: www.elsevier.com/locate/apradiso

# Photons fluence to local skin Dose coefficients and benchmark with three Monte-Carlo codes. Application to the computation of radioactive material transport limits

Thomas Frosio [a,*], Philippe Bertreix [a], Nabil Menaa [a], Samuel Thomas [b], Holger Eberhardt [c], Janis Endres [c]

[a] Radiation Protection Group, European Organization for Nuclear Research, 1211, Geneva 23, Switzerland
[b] Institut de Radioprotection et de Sûreté Nucléaire, 92260, Fontenay-aux-Roses, France
[c] Gesellschaft für Anlagen- und Reaktorsicherheit gGmbH, 50667, Cologne, Germany

ARTICLE INFO

*Keywords:*
GEANT4
FLUKA
MCNP
Fluence to Local-Skin-Dose conversion coefficients
Photon radiations
Monte-Carlo simulations
Transport of radioactive material

ABSTRACT

Fluence to Local Skin Dose Conversion Coefficients (LSD-CC) are radiological protection quantities used for external radiation exposures which allow the conversion of particle fluences into local skin equivalent dose. The International Commission on Radiological Protection published LSD-CC for electrons with an energy range from 10 keV to 10 MeV. However, the literature does not address these radiation protection quantities for all particle types, in particular for photons. In this article, computed LSD-CC values for photons are presented which enrich the literature and are of interest for the radiation protection community. As an example for an application of the use of the computed LSD-CC values, the IAEA A1/A2 working group, which supports the review of the international regulation related to the transport of radioactive material, has decided to estimate the dose to the skin using such coefficients. In this publication, LSD-CC for photons are computed and benchmarked using GEANT4, FLUKA and MCNP. In addition, the FLUKA Monte-Carlo calculation code is used to compute the LSD-CC values for electrons and positrons to compare with existing data in the literature and validate the presented models. As one application of these LSD-CC values, the transfer functions for calculating the IAEA A-values are determined using the LSD-CC and are compared to a one-step direct calculation method.

## 1. Introduction

Estimation of organ dose due to electrons, positrons, and photons is of high interest for radiation protection purposes. ICRP publication 116 (ICRP116, 2010) defines a set of organ protection quantities. Among these protection quantities, the so called "Local Skin Dose" (LSD) represents the dose of the epidermis in skin. ICRP publication 116 (ICRP116, 2010) reports LSD Conversion Coefficients (LSD-CC) for electrons and alpha particles only. Such coefficients are multiplied with particle fluences to construct the LSD protection quantity. The LSD-CC values for photons and positrons are missing in ICRP publication 116 (ICRP116, 2010) for such protection quantities. In this paper, a calculation method based on three Monte Carlo simulation codes to extend the LSD-CC values for photons is proposed. A set of LSD-CC values is also produced and respectively compared with the values of ICRP publication 116 for electrons and (BOURGOIS, 2016) for positrons to ensure the correctness of the presented calculation method.

One application of using the computed LSD-CC values is the establishment of the activity limit values for the safe transport of radioactive material following the methodology (Q-system) defined in IAEA's (International Atomic Energy Agency) publication SSG-26 (IAEASSG26, 2012) for calculating A-values. A dedicated working group (WG) has been created, under the IAEA TRANSSC (Transport Safety Standards Committee) supervision, to review and update the methodology for calculating the activity limits (A-values). Within the WG, the skin dose for a person exposed in transport accident scenario is estimated by convoluting the LSD Conversion Coefficients (LSD-CC) with the particles fluence obtained in the air at 1 m distance from a radioactive source (IAEASSG26, 2012). This quantity is named "$Q_B$". The result of such a convolution is called "transfer function" in this article (FROSIO et al., 2020).

In order to evaluate the effect of LSD-CC in the establishment of the

* Corresponding author.
*E-mail address:* Thomas.frosio@gmail.com (T. Frosio).

https://doi.org/10.1016/j.apradiso.2021.109892
Received 25 May 2021; Received in revised form 8 August 2021; Accepted 8 August 2021
Available online 14 August 2021

**Table 1**
Skin elemental composition mass percent.

| Element | Composition (Mass %) | Density (g/cm$^3$) |
|---|---|---|
| Hydrogen | 10.0 | 1.09 |
| Carbon | 19.9 | |
| Nitrogen | 4.2 | |
| Oxygen | 65.0 | |
| Sodium | 0.2 | |
| Phosphorus | 0.1 | |
| Sulfur | 0.2 | |
| Chlorine | 0.3 | |
| Potassium | 0.1 | |

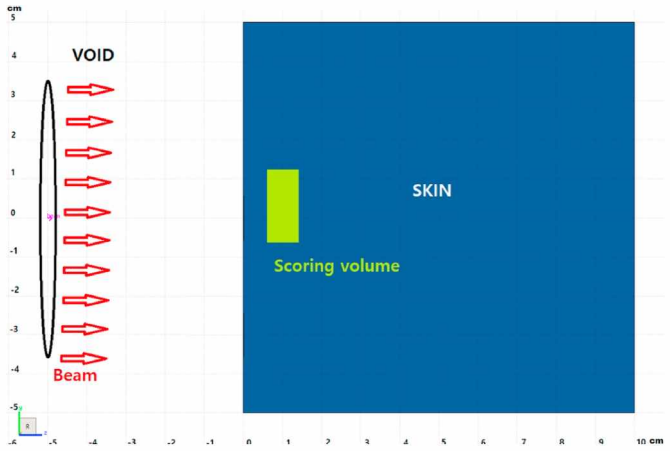


**Fig. 1.** Geometry model for the computation of LSD per fluence conversion coefficients. The scoring volume is not to scale.

transfer function, a one-step calculation method of the $Q_B$ quantity is performed to estimate the local-skin dose directly, without the use of the LSD-CC values, as it was previously the case in the WG (TFR19, 2019). Both constructions (LSD-CC based and one-step methods) are compared.

Section 2 describes the calculation model used to establish the LSD-CC values. It also presents the results obtained, and the comparison with values available in the literature. Section 3 aims at presenting the "transfer function" determination method and comparing the one constructed with the LSD-CC values to the one-step calculation technique.

## 2. LSD per fluence conversion coefficients

The calculation of LSD per fluence coefficients, are assessed using the Monte-Carlo code FLUKA 2011.3 (FLUKA14 et al., 2014) (FLUKA15 et al., 2015) with FLAIR (Vlachoudis, 2009), GEANT4.10.6 (S. Agostinelli et al. Geant4—a simulation toolkit, 2003) (J. Allison et al. Recent developments in Geant4, 2016) and MCNP6.2 (Werner, 2017) (C. J. Werner et al. MCNP6.2 release notes., 2018). The simulation geometry is detailed in the next subsection.

### 2.1. LSD geometry

Annex G of (ICRP116, 2010) defines the geometry to determine the LSD-CC values via Monte-Carlo simulations. It consists of a circular parallel beam with a diameter of 7 cm diameter of mono-energetic particles in a vacuum, normally incident on a 10x10x10 cm$^3$ skin cube. The elemental composition of the skin is defined in table B1 of (ICRP110, 2009) and is summarized in Table 1.

In this specific case of electrons, positrons, and photons, the radiation weighting factor is set to a value of 1 (ICRP92, 2003). Consequently, in what follows, the word "dose" refers to either the absorbed or the equivalent dose interchangeably.

The dose is scored over a cylinder of 1 cm$^2$ surface, with a thickness of 50 μm. The cylinder is geometrically centered on the normal axis of the exposed skin cube side and set back at a depth of 50 μm. This geometry is also used in (BOURGOIS, 2016) for determining LSD-CC values for positrons. The geometry is shown in Fig. 1.

For each primary beam type (electron, positron and photon), the total averaged energy deposited over the scoring volume by all particle types (photon, electron and positrons) is obtained in GeV/g or MeV/g per incident particle. This quantity is converted into an absorbed dose in pGy. Finally, the result is divided by the fluence of the beam (hence it is multiplied by the surface of the source), to get an LSD conversion coefficient per fluence values (LSD-CC) in pGy.cm$^2$, here equivalent to pSv.cm$^2$.

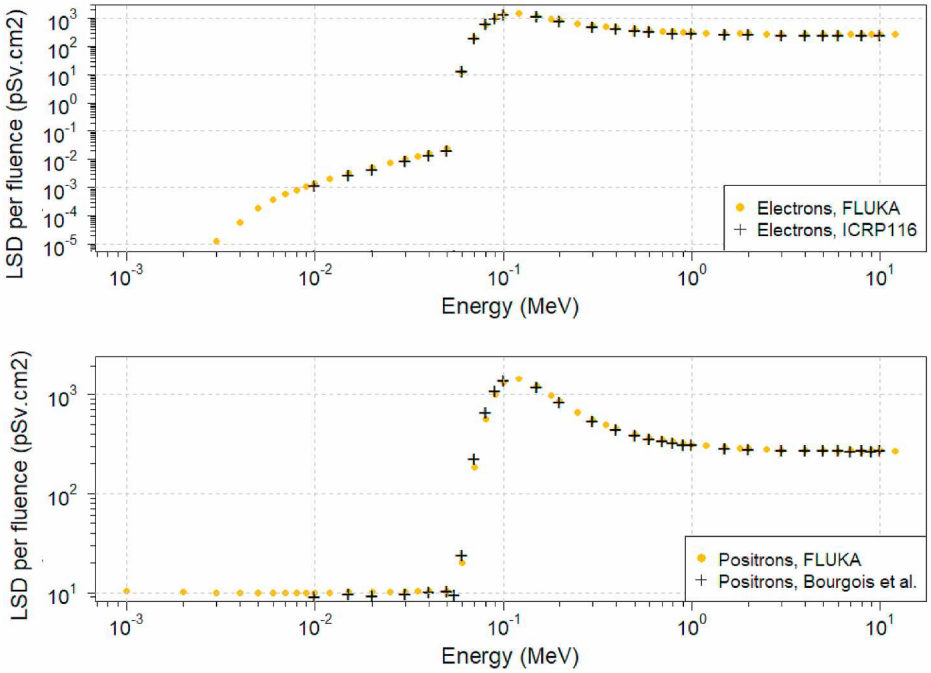


**Fig. 2.** Fluence-LSD conversion coefficients for mono-energetic electrons and positrons.

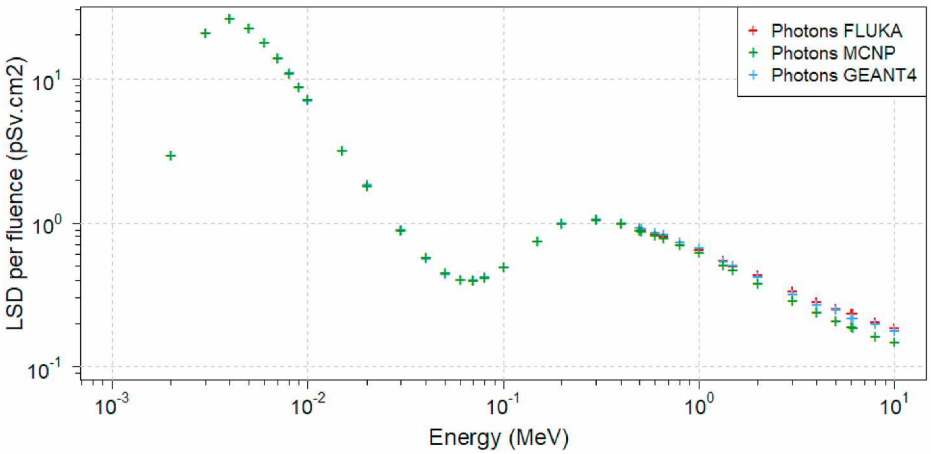


**Fig. 3.** Fluence-LSD conversion coefficients for mono-energetic photons. Comparison with the three Monte-Carlo codes FLUKA, GEANT4 and MCNP. Statistical uncertainties below 2%.

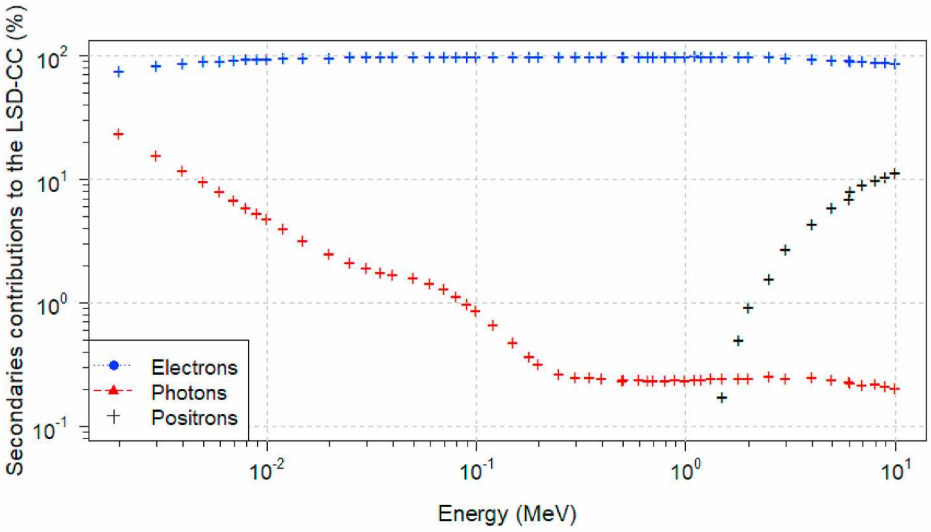


**Fig. 4.** Contributions of secondary particles to the photon LSD-CC value. Calculation obtained with FLUKA.

### 2.2. Calculation codes

FLUKA (FLUKA14 et al., 2014) (FLUKA15 et al., 2015) is a Monte-Carlo simulation code for interaction and transport of multiple particles types, developed at CERN. The physics implemented in FLUKA is available in the FLUKA's manual.[1] For electrons and positrons transport, differences are taken into account for both stopping power and Bremsstrahlung. Regarding photon interactions, FLUKA models include Rayleigh and Compton scattering, photoelectric absorption and pair production. The Monte-Carlo simulation code is used to simulate mono-energetic electrons, photons and positrons, with energy from 1 keV to 10 MeV.

The GEANT4 toolkit (S. Agostinelli et al. Geant4—a simulation toolkit, 2003) (J. Allison et al. Recent developments in Geant4, 2016) is a multipurpose Monte-Carlo code developed through the GEANT4 collaboration. The stopping powers of electrons and positrons are calculated differently providing specific values for both particles. The QGSP_BIC physics is used with the electromagnetic option 4 (EMZ). This option is recommended for performance studies as it is the combination of the most accurate electromagnetic models available in GEANT4. In this study, GEANT4 is used to simulate LSD-CC for photons with energy from 1 keV to 10 MeV.

MCNP6.2 (Werner, 2017) (C. J. Werner et al. MCNP6.2 release notes., 2018) is a Monte-Carlo code developed at Argonne National Laboratory. In this study, MCNP6.2 is used to simulate LSD-CC for photons with energy from 1 keV to 10 MeV. Contrary to the two previous codes, electrons and positrons transport are similar except for positron annihilation (BOURGOIS, 2016) (Werner, 2017) (Tutt et al., 2016). Coherent Thomson scattering and generation of electrons in MODE E are turned on.

In all the three simulation codes, the energy threshold for the production and the transport of electrons, positrons, and photons has been fixed to 1 keV and the secondary photons, electrons and positrons are simulated. Statistical uncertainties are below 2%.

### 2.3. LSD-CC results

The LSD-CC curves are shown in Fig. 2 for electrons, positrons, and photons. The LSD-CC values for electrons, generated with FLUKA only, are compared to the values presented in ICRP 116 (ICRP116, 2010), while the positron values, generated with FLUKA only, are compared to the works of (BOURGOIS, 2016). The results show quantitative and qualitative agreements.

[1] https://flukafiles.web.cern.ch/manual/INDEX-fluka.html.

**Table 2**
Fluence-LSD conversion factors for mono-energetic electrons and positrons. Comparison with ICRP 116 for electrons and with Bourgois et al. for positrons. The radiation weighting factor being 1, values can be understood as pSv.cm$^2$ or pGy.cm$^2$.

| This work | | | ICRP 116 | Bourgois et al. | Ratio | |
|---|---|---|---|---|---|---|
| Energy | Electrons FLUKA | Positrons FLUKA | Electrons | Positrons | This work/ICRP116 | This work/Bourgois |
| (MeV) | pSv.cm$^2$ or pGy. cm$^2$ | pSv.cm$^2$ or pGy. cm$^2$ | pSv.cm$^2$ | pSv.cm$^2$ | pSv.cm$^2$ | pSv.cm$^2$ |
| 0.001 | 0.00 | 1.04 $10^{1}$ | – | – | – | – |
| 0.002 | 0.00 | 1.01 $10^{1}$ | – | – | – | – |
| 0.003 | 1.21 $10^{-5}$ | 1.00 $10^{1}$ | – | – | – | – |
| 0.004 | 5.95 $10^{-5}$ | 9.98 | – | – | – | – |
| 0.005 | 1.88 $10^{-4}$ | 1.00 $10^{1}$ | – | – | – | – |
| 0.006 | 3.76 $10^{-4}$ | 1.00 $10^{1}$ | – | – | – | – |
| 0.007 | 5.75 $10^{-4}$ | 9.96 | – | – | – | – |
| 0.008 | 8.08 $10^{-4}$ | 1.00 $10^{1}$ | – | – | – | – |
| 0.009 | 1.11 $10^{-3}$ | 9.94 | – | – | – | – |
| 0.01 | 1.41 $10^{-3}$ | 1.00 $10^{1}$ | *1.22* $10^{-3}$ | *9.18* | 1.15 | 1.09 |
| 0.012 | 2.10 $10^{-3}$ | 1.00 $10^{1}$ | – | – | – | – |
| 0.015 | 3.16 $10^{-3}$ | 1.01 $10^{1}$ | *2.80* $10^{-3}$ | *9.84* | 1.13 | 1.02 |
| 0.02 | 5.25 $10^{-3}$ | 1.01 $10^{1}$ | *4.73* $10^{-3}$ | *9.43* | 1.11 | 1.07 |
| 0.025 | 7.57 $10^{-3}$ | 1.02 $10^{1}$ | – | – | – | – |
| 0.03 | 1.01 $10^{-2}$ | 1.02 $10^{1}$ | *8.85* $10^{-3}$ | *9.73* | 1.14 | 1.05 |
| 0.035 | 1.29 $10^{-2}$ | 1.03 $10^{1}$ | – | – | – | – |
| 0.04 | 1.63 $10^{-2}$ | 1.03 $10^{1}$ | *1.47* $10^{-2}$ | *1.03* $10^{1}$ | 1.11 | 1.00 |
| 0.05 | 2.34 $10^{-2}$ | 1.04 $10^{1}$ | *2.10* $10^{-2}$ | *1.04* $10^{1}$ | 1.12 | 1.00 |
| 0.06 | 1.22 $10^{1}$ | 2.00 $10^{1}$ | *1.37* $10^{1}$ | *2.43* $10^{1}$ | 0.89 | 0.82 |
| 0.07 | 1.96 $10^{2}$ | 1.86 $10^{2}$ | *2.15* $10^{2}$ | *2.30* $10^{2}$ | 0.91 | 0.81 |
| 0.08 | 5.91 $10^{2}$ | 5.69 $10^{2}$ | *6.62* $10^{2}$ | *6.65* $10^{2}$ | 0.89 | 0.86 |
| 0.09 | 1.03 $10^{3}$ | 1.01 $10^{3}$ | *1.08* $10^{3}$ | *1.10* $10^{3}$ | 0.96 | 0.92 |
| 0.1 | 1.32 $10^{3}$ | 1.33 $10^{3}$ | *1.40* $10^{3}$ | *1.41* $10^{3}$ | 0.95 | 0.94 |
| 0.12 | 1.43 $10^{3}$ | 1.46 $10^{3}$ | – | – | – | – |
| 0.15 | 1.21 $10^{3}$ | 1.23 $10^{3}$ | *1.21* $10^{3}$ | *1.22* $10^{3}$ | 1.00 | 1.01 |
| 0.18 | 9.66 $10^{2}$ | 9.86 $10^{2}$ | – | – | – | – |
| 0.2 | 8.47 $10^{2}$ | 8.62 $10^{2}$ | *8.41* $10^{2}$ | *8.46* $10^{2}$ | 1.01 | 1.02 |
| 0.25 | 6.54 $10^{2}$ | 6.64 $10^{2}$ | – | – | – | – |
| 0.3 | 5.53 $10^{2}$ | 5.58 $10^{2}$ | *5.38* $10^{2}$ | *5.54* $10^{2}$ | 1.03 | 1.01 |
| 0.35 | 4.90 $10^{2}$ | 4.95 $10^{2}$ | – | – | – | – |
| 0.4 | 4.49 $10^{2}$ | 4.53 $10^{2}$ | *4.41* $10^{2}$ | *4.47* $10^{2}$ | 1.02 | 1.01 |
| 0.5 | 3.97 $10^{2}$ | 3.99 $10^{2}$ | *3.82* $10^{2}$ | *3.94* $10^{2}$ | 1.04 | 1.01 |
| 0.6 | 3.67 $10^{2}$ | 3.69 $10^{2}$ | *3.43* $10^{2}$ | *3.64* $10^{2}$ | 1.07 | 1.01 |
| 0.7 | 3.46 $10^{2}$ | 3.48 $10^{2}$ | - | *3.43* $10^{2}$ | – | 1.02 |
| 0.8 | 3.32 $10^{2}$ | 3.33 $10^{2}$ | *3.15* $10^{2}$ | *3.32* $10^{2}$ | 1.06 | 1.00 |
| 0.9 | 3.21 $10^{2}$ | 3.23 $10^{2}$ | | *3.18* $10^{2}$ | | 1.02 |
| 1 | 3.13 $10^{2}$ | 3.15 $10^{2}$ | *3.04* $10^{2}$ | *3.15* $10^{2}$ | 1.03 | 1.00 |
| 1.2 | 3.01 $10^{2}$ | 3.03 $10^{2}$ | – | – | – | – |
| 1.5 | 2.91 $10^{2}$ | 2.92 $10^{2}$ | *2.84* $10^{2}$ | *2.93* $10^{2}$ | 1.03 | 0.99 |
| 1.8 | 2.85 $10^{2}$ | 2.86 $10^{2}$ | – | - | | |
| 2 | 2.82 $10^{2}$ | 2.84 $10^{2}$ | *2.80* $10^{2}$ | *2.86* $10^{2}$ | 1.01 | 0.99 |
| 2.5 | 2.78 $10^{2}$ | 2.79 $10^{2}$ | – | – | – | – |
| 3 | 2.75 $10^{2}$ | 2.77 $10^{2}$ | *2.64* $10^{2}$ | *2.79* $10^{2}$ | 1.04 | 0.99 |
| 4 | 2.74 $10^{2}$ | 2.73 $10^{2}$ | *2.59* $10^{2}$ | *2.78* $10^{2}$ | 1.06 | 0.98 |
| 5 | 2.72 $10^{2}$ | 2.73 $10^{2}$ | *2.59* $10^{2}$ | *2.77* $10^{2}$ | 1.05 | 0.98 |
| 6 | 2.72 $10^{2}$ | 2.71 $10^{2}$ | *2.59* $10^{2}$ | *2.75* $10^{2}$ | 1.05 | 0.99 |
| 7 | 2.72 $10^{2}$ | 2.72 $10^{2}$ | – | *2.74* $10^{2}$ | – | 0.99 |
| 8 | 2.72 $10^{2}$ | 2.71 $10^{2}$ | *2.67* $10^{2}$ | *2.76* $10^{2}$ | 1.02 | 0.98 |
| 9 | 2.72 $10^{2}$ | 2.72 $10^{2}$ | – | *2.74* $10^{2}$ | – | 0.99 |
| 10 | 2.72 $10^{2}$ | 2.72 $10^{2}$ | *2.62* $10^{2}$ | *2.76* $10^{2}$ | 1.04 | 0.98 |

As a purpose of benchmark, LSD-CC for photons are generated with the three Monte-Carlo codes GEANT4, MCNP and FLUKA. Fig. 3 below illustrates the results obtained. A quantitative agreement between the three codes from 1 keV to 200 keV with less than 1% relative difference is observed. From 200 keV to 2 MeV, the relative difference reaches a maximum value of 7%, still compatible with the statistical uncertainty. Above 2 MeV, the relative differences reach a maximum value of 18% between GEANT4 and MCNP; 26% between MCNP and FLUKA; 8% between FLUKA and GEANT4. At energies above 1 MeV, the contribution of secondary positrons to the photon dose cannot be neglected. The differences could then originate from the fact that MCNP considers the same stopping power for electrons and positrons while GEANT4 and FLUKA have specific values for each particle (Vagena et al., 2020). This effect is illustrated in Fig. 4.

Table 2 reports the values obtained in this work with FLUKA for electrons and positrons, as well as from (ICRP116, 2010) and (BOURGOIS, 2016). The ratios are in the range [0.89–1.15] with the ICRP values (for electrons) and [0.81–1.09] with the Bourgois values (positrons). Statistical uncertainties from the numerical simulations are all below 2%. These slight differences cannot be explained by the geometry or mass balance as they are all similar. However, calculations from (BOURGOIS, 2016) and (ICRP116, 2010) have been performed with MCNP (Werner, 2017), hence the physics models and nuclear databases differences could explain the previously mentioned ratios between our

**Table 3**
Fluence-LSD conversion factors for mono-energetic photons obtained with FLUKA, MCNP and GEANT4. Comparison with ICRP 116 for electrons and with Bourgois et al. for positrons. The radiation weighting factor being 1, values can be understood as pSv.cm$^2$ or pGy.cm$^2$.

| LSD-CC photons | FLUKA | MCNP | GEANT4 |
|---|---|---|---|
| Energy (MeV) | Local skin dose (pGy cm$^2$) | Local skin dose (pGy cm$^2$) | Local skin dose (pGy cm$^2$) |
| 0.002 | 2.98 | 2.97 | 2.97 |
| 0.003 | 2.09 $10^1$ | 2.09 $10^1$ | 2.09 $10^1$ |
| 0.004 | 2.63 $10^1$ | 2.63 $10^1$ | 2.63 $10^1$ |
| 0.005 | 2.27 $10^1$ | 2.26 $10^1$ | 2.27 $10^1$ |
| 0.006 | 1.79 $10^1$ | 1.79 $10^1$ | 1.80 $10^1$ |
| 0.007 | 1.40 $10^1$ | 1.40 $10^1$ | 1.41 $10^1$ |
| 0.008 | 1.10 $10^1$ | 1.10 $10^1$ | 1.11 $10^1$ |
| 0.009 | 8.85 | 8.85 | 8.83 |
| 0.01 | 7.22 | 7.22 | 7.20 |
| 0.02 | 3.23 | 3.22 | 3.24 |
| 0.02 | 1.85 | 1.84 | 1.87 |
| 0.03 | 8.97 $10^{-1}$ | 8.86 $10^{-1}$ | 9.01 $10^{-1}$ |
| 0.04 | 5.77 $10^{-1}$ | 5.78 $10^{-1}$ | 5.73 $10^{-1}$ |
| 0.05 | 4.50 $10^{-1}$ | 4.54 $10^{-1}$ | 4.45 $10^{-1}$ |
| 0.06 | 4.06 $10^{-1}$ | 4.06 $10^{-1}$ | 4.08 $10^{-1}$ |
| 0.07 | 4.03 $10^{-1}$ | 4.02 $10^{-1}$ | 4.04 $10^{-1}$ |
| 0.08 | 4.22 $10^{-1}$ | 4.21 $10^{-1}$ | 4.27 $10^{-1}$ |
| 0.10 | 4.95 $10^{-1}$ | 4.93 $10^{-1}$ | 4.96 $10^{-1}$ |
| 0.15 | 7.53 $10^{-1}$ | 7.48 $10^{-1}$ | 7.52 $10^{-1}$ |
| 0.20 | 1.01 | 1.01 | 1.02 |
| 0.30 | 1.08 | 1.07 | 1.09 |
| 0.40 | 9.91 $10^{-1}$ | 9.82 $10^{-1}$ | 1.02 |
| 0.50 | 9.31 $10^{-1}$ | 8.88 $10^{-1}$ | 9.33 $10^{-1}$ |
| 0.51 | 9.08 $10^{-1}$ | 8.79 $10^{-1}$ | 9.12 $10^{-1}$ |
| 0.60 | 8.43 $10^{-1}$ | 8.26 $10^{-1}$ | 8.62 $10^{-1}$ |
| 0.66 | 8.09 $10^{-1}$ | 7.87 $10^{-1}$ | 8.32 $10^{-1}$ |
| 0.80 | 7.38 $10^{-1}$ | 7.11 $10^{-1}$ | 7.41 $10^{-1}$ |
| 1.00 | 6.52 $10^{-1}$ | 6.20 $10^{-1}$ | 6.71 $10^{-1}$ |
| 1.33 | 5.48 $10^{-1}$ | 5.13 $10^{-1}$ | 5.45 $10^{-1}$ |
| 1.50 | 5.05 $10^{-1}$ | 4.77 $10^{-1}$ | 5.08 $10^{-1}$ |
| 2.00 | 4.36 $10^{-1}$ | 3.82 $10^{-1}$ | 4.24 $10^{-1}$ |
| 3.00 | 3.40 $10^{-1}$ | 2.90 $10^{-1}$ | 3.21 $10^{-1}$ |
| 4.00 | 2.87 $10^{-1}$ | 2.42 $10^{-1}$ | 2.71 $10^{-1}$ |
| 5.00 | 2.55 $10^{-1}$ | 2.10 $10^{-1}$ | 2.54 $10^{-1}$ |
| 6.00 | 2.39 $10^{-1}$ | 1.91 $10^{-1}$ | 2.21 $10^{-1}$ |
| 6.13 | 2.37 $10^{-1}$ | 1.88 $10^{-1}$ | 2.19 $10^{-1}$ |
| 8.00 | 2.08 $10^{-1}$ | 1.64 $10^{-1}$ | 2.00 $10^{-1}$ |
| 10.00 | 1.90 $10^{-1}$ | 1.50 $10^{-1}$ | 1.79 $10^{-1}$ |

results and those from Bourgois and ICRP116. Table 3 provides LSD-CC values for photons as obtained with GEANT4, MCNP and FLUKA.

## 3. Application to the transport of radioactive materials: transfer function for $Q_B$ scenario

IAEA SSG26 (IAEASSG26, 2012) defines the irradiation scenario for the calculation of the activity limits (A-values). In particular, one of the scenarios, named "$Q_B$", defines the skin dose of a person exposed following an accident involving a type A transport package.

The recent discussions in the IAEA A1/A2 WG focused among other topics on improving the determination of $Q_B$. The $Q_B$ quantity is planned to be extended to all kinds of radiations[2] emitted by radionuclide decays. It would no longer be limited to beta (or electron) emissions such as in (IAEASSG26, 2012). Moreover, it is planned to use LSD-CC values for the computation of this updated $Q_B$.

Two methods are compared to construct the transfer function: one referred to as "Protection quantity" because it relies on the LSD-CC values as defined in ICRP 116, and the second referred to as "direct calculation" because the transfer function is computed in one calculation step. These methods are further detailed below. They reflect two different approaches to model the same problem, and therefore differences in results are expected. Calculations are performed with the FLUKA Monte Carlo code and the LSD-CC values considered are those obtained with FLUKA and described in this document for electrons, positrons and photons. The choice of considering only FLUKA is here to avoid overloading the paper with a lot of results that would be quite similar for the three codes as shown in Fig. 3. Furthermore, FLUKA provides penalizing results at high energy (Fig. 3), where discrepancies between the three codes are obtained.

The determination of the transfer functions representative of the updated $Q_B$ scenario is performed using Monte-Carlo simulations and geometry models as detailed in Fig. 5 for both methods (LSD-CC and direct). Simulations are done for each particle type (electron, positron and photon) at different energies, as presented below in section 3.1.

### 3.1. Geometry of irradiation

The geometry used for both transfer function determination methods are described in Fig. 5 below.


**Fig. 5.** Geometry representation of the fluences simulation for $Q_B$ scenario. Left figure presents the protection quantity calculation (LSD-CC method). Right figure describes the direct calculation method.

[2] Communication with the working group.

**Table 4**
Steel316L elemental composition in mass percent (PNNL, 2011).

| Element | Composition (Mass %) | Density (g/cm$^3$) |
|---|---|---|
| Carbon | 0.03 | 8.0 |
| Silicon | 1.0 | |
| Phosphorus | 0.045 | |
| Sulfur | 0.03 | |
| Chromium | 17.0 | |
| Manganese | 2.0 | |
| Iron | 65.395 | |
| Nickel | 12.0 | |
| Molybdenum | 2.5 | |

### 3.1.1. *Method 1: protection quantity method, WG agreed choice*

To determine the particles fluences crossing the skin surface, an isotropic point source of electrons, positrons or photons is located at the centre of the geometry. The source is encapsulated in a sphere of Steel316L (WG agreed choice, see Table 4), whose elemental composition is defined in PNNL (PNNL, 2011). The WG agrees that the steel is representative of the remaining part of the package that would not have been destroyed in the accident. Fluences are scored at 1 m from the source in the air.

The transfer function (TFR19, 2019) (TFR20, 2020) $\top_p(\mathrm{E})$ converts radionuclide decay emissions into an equivalent skin dose in the updated $Q_B$ scenario ($H_{Q_B}$). It is computed for a radionuclide emission at energy E and particle p by the following integral:

$$\top_p(\mathrm{E}) = \sum_{p'} \int \Phi_{E,p}(E', p')\mathrm{LSDCC}(E', p')dE'$$

Where $\Phi_{E,p}(E', p')$ is the fluence of particles $p'$ (described in Fig. 5, left part) at energy $E'$ originating from incident particles $p$ emitted at energy $E$ at 1 m from the source. $\mathrm{LSDCC}(E', p')$ is the LSD per fluence coefficient,

**Table 5**
Transfer functions for local skin dose calculation ($Q_B$) considering electrons, positrons and photons radiations. Comparison with one-step method. Results obtained with FLUKA.

| Energy (MeV) | Electrons Sv/h per primary/s | | Sv/h per primary/s | | Sv/h per primary/s | |
|---|---|---|---|---|---|---|
| | ⊤ direct | ⊤ protection | ⊤ direct | ⊤ protection | ⊤ direct | ⊤ protection |
| 0.001 | 0.00 | 0.00 | 2.28 10$^{-13}$ | 2.09 10$^{-13}$ | 0.00 | 0.00 |
| 0.002 | 0.00 | 0.00 | 2.29 10$^{-13}$ | 2.09 10$^{-13}$ | 0.00 | 0.00 |
| 0.003 | 0.00 | 0.00 | 2.29 10$^{-13}$ | 2.09 10$^{-13}$ | 0.00 | 0.00 |
| 0.004 | 0.00 | 0.00 | 2.30 10$^{-13}$ | 2.09 10$^{-13}$ | 0.00 | 0.00 |
| 0.005 | 0.00 | 0.00 | 2.28 10$^{-13}$ | 2.09 10$^{-13}$ | 0.00 | 0.00 |
| 0.006 | 0.00 | 0.00 | 2.29 10$^{-13}$ | 2.09 10$^{-13}$ | 0.00 | 0.00 |
| 0.007 | 0.00 | 0.00 | 2.29 10$^{-13}$ | 2.08 10$^{-13}$ | 0.00 | 0.00 |
| 0.008 | 0.00 | 0.00 | 2.30 10$^{-13}$ | 2.08 10$^{-13}$ | 0.00 | 0.00 |
| 0.009 | 0.00 | 0.00 | 2.29 10$^{-13}$ | 2.09 10$^{-13}$ | 0.00 | 0.00 |
| 0.01 | 0.00 | 0.00 | 2.30 10$^{-13}$ | 2.08 10$^{-13}$ | 0.00 | 0.00 |
| 0.01 | 0.00 | 0.00 | 2.29 10$^{-13}$ | 2.09 10$^{-13}$ | 0.00 | 0.00 |
| 0.02 | 0.00 | 0.00 | 2.29 10$^{-13}$ | 2.09 10$^{-13}$ | 0.00 | 8.13 10$^{-23}$ |
| 0.02 | 0.00 | 0.00 | 2.31 10$^{-13}$ | 2.08 10$^{-13}$ | 2.09 10$^{-18}$ | 1.75 10$^{-18}$ |
| 0.03 | 0.00 | 8.22 10$^{-22}$ | 2.29 10$^{-13}$ | 2.09 10$^{-13}$ | 1.82 10$^{-16}$ | 1.47 10$^{-16}$ |
| 0.03 | 0.00 | 1.64 10$^{-20}$ | 2.30 10$^{-13}$ | 2.08 10$^{-13}$ | 1.39 10$^{-15}$ | 1.00 10$^{-15}$ |
| 0.04 | 1.27 10$^{-19}$ | 9.54 10$^{-20}$ | 2.29 10$^{-13}$ | 2.08 10$^{-13}$ | 3.99 10$^{-15}$ | 2.56 10$^{-15}$ |
| 0.04 | 4.06 10$^{-19}$ | 2.94 10$^{-19}$ | 2.28 10$^{-13}$ | 2.09 10$^{-13}$ | 7.22 10$^{-15}$ | 4.10 10$^{-15}$ |
| 0.05 | 1.85 10$^{-18}$ | 1.17 10$^{-18}$ | 2.29 10$^{-13}$ | 2.09 10$^{-13}$ | 1.35 10$^{-14}$ | 6.31 10$^{-15}$ |
| 0.06 | 4.59 10$^{-18}$ | 2.68 10$^{-18}$ | 2.28 10$^{-13}$ | 2.09 10$^{-13}$ | 1.80 10$^{-14}$ | 7.72 10$^{-15}$ |
| 0.07 | 8.93 10$^{-18}$ | 4.83 10$^{-18}$ | 2.29 10$^{-13}$ | 2.08 10$^{-13}$ | 2.22 10$^{-14}$ | 8.96 10$^{-15}$ |
| 0.08 | 1.47 10$^{-17}$ | 7.53 10$^{-18}$ | 2.30 10$^{-13}$ | 2.09 10$^{-13}$ | 2.51 10$^{-14}$ | 1.03 10$^{-14}$ |
| 0.09 | 2.18 10$^{-17}$ | 1.09 10$^{-17}$ | 2.29 10$^{-13}$ | 2.09 10$^{-13}$ | 2.82 10$^{-14}$ | 1.19 10$^{-14}$ |
| 0.10 | 2.99 10$^{-17}$ | 1.46 10$^{-17}$ | 2.29 10$^{-13}$ | 2.09 10$^{-13}$ | 3.11 10$^{-14}$ | 1.33 10$^{-14}$ |
| 0.12 | 5.00 10$^{-17}$ | 2.40 10$^{-17}$ | 2.29 10$^{-13}$ | 2.09 10$^{-13}$ | 3.60 10$^{-14}$ | 1.67 10$^{-14}$ |
| 0.15 | 8.96 10$^{-17}$ | 4.17 10$^{-17}$ | 2.29 10$^{-13}$ | 2.09 10$^{-13}$ | 4.33 10$^{-14}$ | 2.13 10$^{-14}$ |
| 0.18 | 1.37 10$^{-16}$ | 6.38 10$^{-17}$ | 2.30 10$^{-13}$ | 2.09 10$^{-13}$ | 5.03 10$^{-14}$ | 2.59 10$^{-14}$ |
| 0.20 | 1.74 10$^{-16}$ | 8.11 10$^{-17}$ | 2.30 10$^{-13}$ | 2.09 10$^{-13}$ | 5.39 10$^{-14}$ | 2.95 10$^{-14}$ |
| 0.25 | 2.80 10$^{-16}$ | 1.32 10$^{-16}$ | 2.31 10$^{-13}$ | 2.09 10$^{-13}$ | 6.33 10$^{-14}$ | 3.89 10$^{-14}$ |
| 0.30 | 4.09 10$^{-16}$ | 1.95 10$^{-16}$ | 2.30 10$^{-13}$ | 2.09 10$^{-13}$ | 7.26 10$^{-14}$ | 5.31 10$^{-14}$ |
| 0.35 | 5.59 10$^{-16}$ | 2.69 10$^{-16}$ | 2.30 10$^{-13}$ | 2.09 10$^{-13}$ | 8.08 10$^{-14}$ | 6.60 10$^{-14}$ |
| 0.40 | 7.14 10$^{-16}$ | 3.56 10$^{-16}$ | 2.30 10$^{-13}$ | 2.10 10$^{-13}$ | 9.15 10$^{-14}$ | 7.83 10$^{-14}$ |
| 0.50 | 1.11 10$^{-15}$ | 5.72 10$^{-16}$ | 2.30 10$^{-13}$ | 2.10 10$^{-13}$ | 1.12 10$^{-13}$ | 1.02 10$^{-13}$ |
| 0.60 | 1.56 10$^{-15}$ | 8.38 10$^{-16}$ | 2.32 10$^{-13}$ | 2.10 10$^{-13}$ | 1.34 10$^{-13}$ | 1.23 10$^{-13}$ |
| 0.70 | 2.10 10$^{-15}$ | 1.17 10$^{-15}$ | 2.33 10$^{-13}$ | 2.11 10$^{-13}$ | 1.52 10$^{-13}$ | 1.43 10$^{-13}$ |
| 0.80 | 2.72 10$^{-15}$ | 1.57 10$^{-15}$ | 2.34 10$^{-13}$ | 2.12 10$^{-13}$ | 1.70 10$^{-13}$ | 1.56 10$^{-13}$ |
| 0.90 | 2.47 10$^{-14}$ | 3.05 10$^{-14}$ | 2.61 10$^{-13}$ | 2.47 10$^{-13}$ | 1.82 10$^{-13}$ | 1.64 10$^{-13}$ |
| 1.00 | 8.36 10$^{-13}$ | 1.04 10$^{-12}$ | 1.19 10$^{-12}$ | 1.39 10$^{-12}$ | 1.91 10$^{-13}$ | 1.70 10$^{-13}$ |
| 1.20 | 7.04 10$^{-12}$ | 7.14 10$^{-12}$ | 7.70 10$^{-12}$ | 7.66 10$^{-12}$ | 2.06 10$^{-13}$ | 1.80 10$^{-13}$ |
| 1.50 | 1.12 10$^{-11}$ | 1.04 10$^{-11}$ | 1.14 10$^{-11}$ | 1.02 10$^{-11}$ | 2.20 10$^{-13}$ | 1.92 10$^{-13}$ |
| 1.80 | 1.12 10$^{-11}$ | 1.04 10$^{-11}$ | 1.11 10$^{-11}$ | 9.94 10$^{-12}$ | 2.20 10$^{-13}$ | 1.91 10$^{-13}$ |
| 2.00 | 1.08 10$^{-11}$ | 1.01 10$^{-11}$ | 1.07 10$^{-11}$ | 9.64 10$^{-12}$ | 2.17 10$^{-13}$ | 1.88 10$^{-13}$ |
| 2.50 | 1.02 10$^{-11}$ | 9.63 10$^{-12}$ | 9.96 10$^{-12}$ | 9.16 10$^{-12}$ | 2.08 10$^{-13}$ | 1.80 10$^{-13}$ |
| 3.00 | 9.67 10$^{-12}$ | 9.38 10$^{-12}$ | 9.68 10$^{-12}$ | 8.97 10$^{-12}$ | 2.01 10$^{-13}$ | 1.76 10$^{-13}$ |
| 4.00 | 9.35 10$^{-12}$ | 9.16 10$^{-12}$ | 9.33 10$^{-12}$ | 8.79 10$^{-12}$ | 1.94 10$^{-13}$ | 1.71 10$^{-13}$ |
| 5.00 | 9.22 10$^{-12}$ | 9.10 10$^{-12}$ | 9.14 10$^{-12}$ | 8.74 10$^{-12}$ | 1.94 10$^{-13}$ | 1.70 10$^{-13}$ |
| 6.00 | 9.05 10$^{-12}$ | 9.05 10$^{-12}$ | 9.07 10$^{-12}$ | 8.75 10$^{-12}$ | 1.96 10$^{-13}$ | 1.72 10$^{-13}$ |
| 7.00 | 9.03 10$^{-12}$ | 9.04 10$^{-12}$ | 9.06 10$^{-12}$ | 8.74 10$^{-12}$ | 1.99 10$^{-13}$ | 1.75 10$^{-13}$ |
| 8.00 | 9.01 10$^{-12}$ | 9.03 10$^{-12}$ | 9.04 10$^{-12}$ | 8.76 10$^{-12}$ | 2.02 10$^{-13}$ | 1.78 10$^{-13}$ |
| 9.00 | 9.02 10$^{-12}$ | 9.03 10$^{-12}$ | 9.02 10$^{-12}$ | 8.77 10$^{-12}$ | 2.04 10$^{-13}$ | 1.82 10$^{-13}$ |
| 10.00 | 8.98 10$^{-12}$ | 9.02 10$^{-12}$ | 9.04 10$^{-12}$ | 8.79 10$^{-12}$ | 2.08 10$^{-13}$ | 1.86 10$^{-13}$ |
| 12.00 | 9.07 10$^{-12}$ | 9.02 10$^{-12}$ | 9.01 10$^{-12}$ | 8.83 10$^{-12}$ | 2.16 10$^{-13}$ | 1.94 10$^{-13}$ |

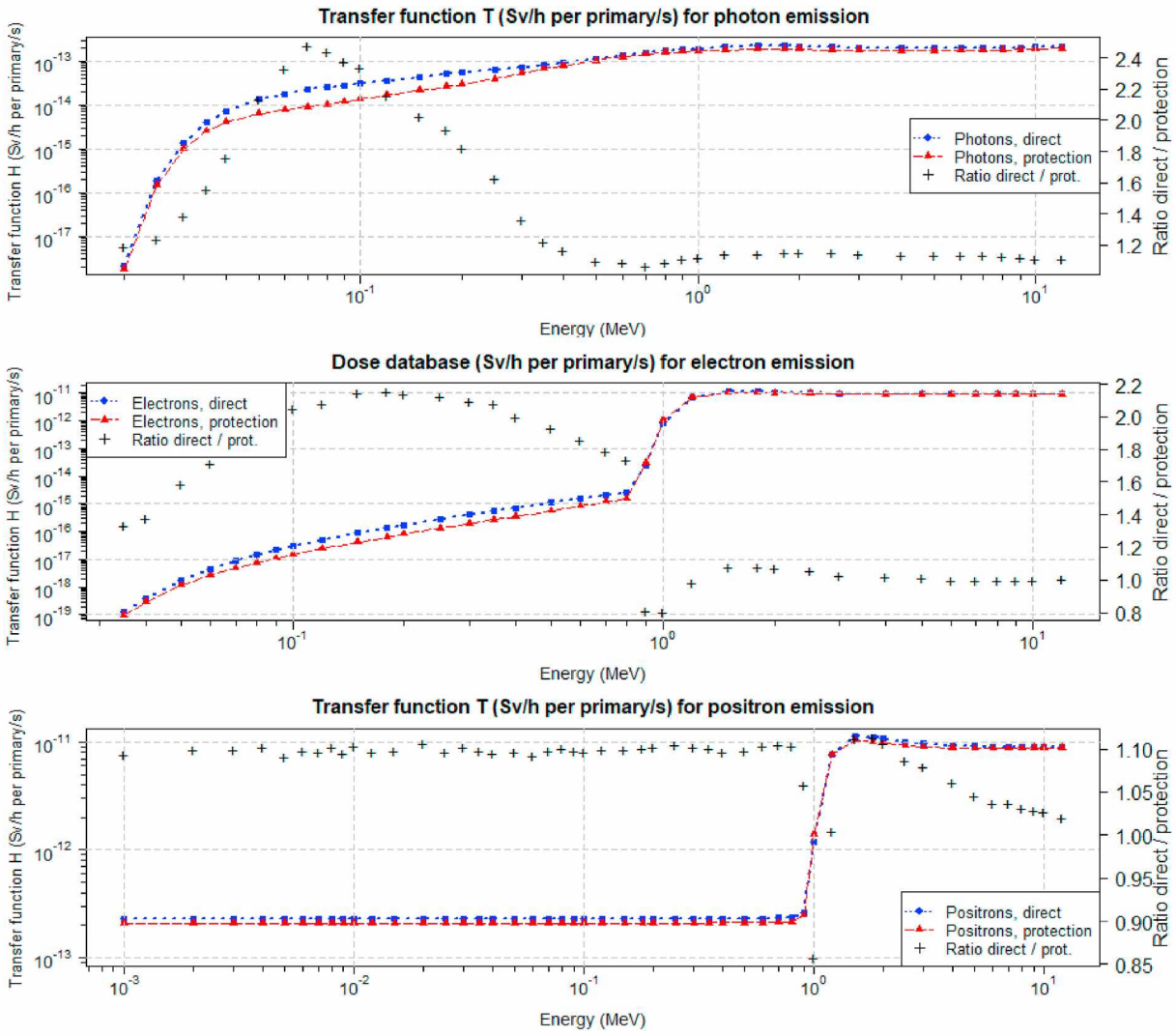


**Fig. 6.** Transfer functions for the computation of transport regulation limits in the case of photons, electrons and positrons radiations. Statistical uncertainties from numerical simulations are below 2%. Results obtained with FLUKA.

which calculation is detailed in section 2 (Fig. 1), for particles $p'$ at energy $E'$.

The equivalent dose in the $Q_B$ scenario $H_{Q_B,rn}$ for a specific radionuclide $rn$ is then obtained as follows:

$$H_{Q_B,rn} = \sum_{p} \top_p(\mathrm{E}) Y_{p,rn}(E) + \int \top_p(\mathrm{E}) \vartheta_{p,rn}(E) dE$$

Where $Y_{p,rn}(E)$ and $\vartheta_{p,rn}(E)$ respectively represent the yield of discrete particle emissions (electrons and photons) and the spectrum of continuous particles (electrons and positrons) emitted by the decay of the radionuclide of interest.

### 3.1.2. Method 2: direct calculation

As for method 1, an isotropic point source of electrons, positrons or photons is located at the center of the geometry, and is encapsulated in a sphere of Steel316L surrounded by a 1-m radius sphere of air. The skin material is modelled to surround the 1 m air sphere. The dose ($H_{Q_B}$) is directly scored at 50 μm depth in the skin with a thickness of 50 μm (Fig. 5, right part). The method 2 was initially used within the WG and in particular described in (TFR19, 2019). For consistency reasons linked to the radiation protection standards, it has recently been decided to use the LSD-CC (method 1).

### 3.2. Transfer functions for skin dose evaluation in updated $Q_B$ scenario - results

This section aims at comparing the transfer functions evaluated for both protection quantity calculation (LSD-CC) and direct calculation. These two different methods have been discussed within the IAEA WG for the revision of the international regulation related to the safe transport of radioactive material. Since the IAEA WG recently opted for using the LSD-CC values to estimate the $Q_B$ quantity, the LSD-CC values had to be computed when they are not available in the literature (section 2). This section describes an application for the use of the completed LSD-CC values that have been calculated in this article. The two methods are driven by different considerations and their differences should be evaluated, as the two methods are not expected to lead to similar results.

Discrepancies between the LSD-CC based protection quantity method and direct method values for the transfer functions are observed. The results of the direct method are slightly above the protection quantity for energies below 500 keV compared to the protection quantity. This overestimation reaches:

- A factor 2.5 for incident photons of 70 keV,
- A factor 2.2 for incident electrons at 200 keV,
- A factor 0.85 for positrons at 1 MeV.

Table 5 reports the transfer function values for the particle types of interest and Fig. 6 illustrates those values, as estimated with both methods. The two methods differ, due to the differences in the numerical simulation geometries assumptions. Indeed, the particles generated in the case of the protection quantity method can travel above 50 μm across the skin without going through the scoring volume, as it is centered in the skin cube (Fig. 1). On the opposite, for the direct calculation method, all the particles that travel above 50 μm depth will go through the scoring volume, due to the sphere geometry (Fig. 5, right part). The direct calculation method has been previously studied by the WG but for consistency reason with the ICRP-116 standard, the LSD-CC method is considered for the $Q_B$ quantity calculation. Furthermore, the LSD-CC method is in general more conservative.

The LSD-CC values are calculated with a lower energy limit of 1 keV while the lower value provided in ICRP116 is 10 keV. Comparisons have been performed to assess the impact of the LSD-CC values below 10 keV on the transfer function. No significant differences were found and therefore it is not presented in this study. The results are impacted only at the second significant digit, which indicates that computation of LSD-CC values below 10 keV is unnecessary for the establishment of the new $Q_B$ values. However, this could be of interest for other applications of LSD per fluence conversion coefficients.

## 4. Conclusions

In this article, LSD per fluence conversion coefficients (LSD-CC) for photons have been computed in order to enrich the literature. For comparison purposes and in order to validate the used computation method, the coefficients for positrons and electrons have also been calculated and compared to available values in the literature. The results presented in this paper are consistent with the values found in the literature, for electrons and positrons. LSD-CC for photons have been computed with three Monte-Carlo calculation codes well known in the radiation protection community. These codes are GEANT4, FLUKA and MCNP. The results agree qualitatively and quantitatively between the three codes. At high energies above 2 MeV, discrepancies are observed and cannot be explained by the statistical uncertainties. However, differences in the electron and positron stopping powers between the codes may explain the observed discrepancies.

The computed LSD-CC values have been used to update the activity limit values (A-values) for the safe transport of radioactive material. The LSD-CC protection quantities are used to estimate the transfer functions for the updated $Q_B$ scenario that converts radionuclide decay emissions to skin dose. This $Q_B$ quantity is significant, among others, in the international regulations for the transport of radioactive material, to evaluate the activity limit A-values for transport of radioactive material. As an example for an application the transfer function, computed by the means of LSD-CC values in order to construct the protection quantity is compared to a one-step direct calculation method. The two methods are consistent for positrons and show differences for electrons and photons in the energy range of 20 keV–1 MeV. Finally, extending the LSD-CC values down to 1 keV has no practical effect (below 1%) on the transfer function value for the $Q_B$ scenario. However, this could be of interest for other applications of LSD per fluence conversion coefficients.

## Declaration of competing interest

The authors declare that they have no known competing financial interests or personal relationships that could have appeared to influence the work reported in this paper.

## Acknowledgments

The authors would like to thank Ina Petrova for her careful review of the article which has enriched its quality.

The work of GRS is founded by the Federal Ministry for the Environment, Nature Conservation and Nuclear Safety, support code 4720E03300.

## References

Agostinelli, S., et al., 2003. Geant4—a simulation toolkit. Nucl. Instrum. Methods Phys. Res. A 506 (Issue 3), 250–303, 1 July 2003.
Allison, J., et al., 2016. Recent developments in Geant4. Nucl. Instrum. Methods Phys. Res. A 835, 186–225, 1 November 2016.
BOURGOIS, 2016. L. BOURGOIS, R. ANTONI. Fluence to local skin absorbed dose and dose equivalent conversion coefficients for monoenergetic positrons using Monte-Carlo code MCNP6. Appl. Radiat. Isot. 107, 372–376, 2016.
FLUKA14, Bohlen, T.T., Cerutti, F., Chin, M.P.W., Fassò, A., Ferrari, A., Ortega, P.G., Mairani, A., Sala, P.R., Smirnov, G., Vlachoudis, V., 2014. The FLUKA code: developments and challenges for high energy and medical applications. Nucl. Data Sheets 120, 211–214, 2014.
FLUKA15, Battistoni, G., Boehlen, T., Cerutti, F., Chin, P.W., Esposito, L.S., Fassò, A., Ferrari, A., Lechner, A., Empl, A., Mairani, A., Mereghetti, A., Garcia Ortega, P., Ranft, J., Roesler, S., Sala, P.R., Vlachoudis, V., Smirnov, G., 2015. Overview of the FLUKA code. Ann. Nucl. Energy 82, 10–18, 2015.
TFR20, Frosio, T., et al., 2020. Computation of radioactive material transport limits within A1/A2 working group at IAEA TRANSSC. IEEE Access 8, 29040–29054.
IAEASSG26, 2012. Advisory Material for the IAEA Regulations for the Safe Transport of Radioactive Material (2012 Edition).
ICRP110, 2009. Adult reference computational phantoms. Ann. ICRP 39 (2).
ICRP116, 2010. Conversion coefficients for radiological protection quantities for external radiation exposures.ICRP Publication 116. Ann. ICRP 40 (2–5).
ICRP92, 2003. Relative biological effectiveness (RBE), quality factor (Q), and radiation weighting factor (wR). ICRP publication 92. Ann. ICRP 33 (4).
PNNL, 2011. Compendium of Material Composition Data for Radiation Transport Modeling.
TFR19, 2019. T. FROSIO et al. Spectrum and yield to dose conversion coefficients for beta skin doses linked to the Q system. Health Phys. 116 (5), 607–618, 2019.
Tutt, J., Mckinney, G., Wilcox, T., 2016. All-Particle Spontaneous-Decay and Delayed-Positron Capabilities in MCNP6. LA-UR-16-23338.
Vagena, E., Androulakaki, E.G., Kokkoris, M., Patronis, N., Stamati, M.E., 2020. A comparative study of stopping power calculations implemented in Monte Carlo codes and compilations with experimental data. Nucl. Instrum. Methods Phys. Res. Sect. B Beam Interact. Mater. Atoms 467, 44–52.
Vlachoudis, V., 2009. V. Vlachoudis. FLAIR: a powerful but user friendly graphical interface for FLUKA. In: Proc. Int. Conf. On Mathematics, Computational Methods & Reactor Physics (M&C 2009), Saratoga Springs, New York, 2009.
Werner, C.J., 2017. MCNP Users Manual - Code Version 6.2. Los Alamos National Laboratory report LA-UR-17-29981.
Werner, C.J., et al., 2018. MCNP6.2 Release Notes. Los Alamos National Laboratory report LA-UR-18-20808.